applied sciences

MDPI

Article

Preparation and Electrochemical Properties of Functionalized Multi-Walled Carbon Nanotubes @ Carbon Quantum Dots @ Polyaniline Ternary Composite Electrode Materials

Jing Wang [1,*], Youyang Chen [1], Zhihao Hu [1], Ye Ge [1], Guotao Dong [1], Tianhao Hu [1] and Chul Gyu Jhun [2,*]

1 School of Materials Science and Engineering, Anhui University of Science and Technology, Huainan 232001, China; 2018200598@aust.edu.cn (Y.C.); 2018200603@aust.edu.cn (Z.H.); 2019200621@aust.edu.cn (Y.G.); 2019200615@aust.edu.cn (G.D.); 2019200620@aust.edu.cn (T.H.)

2 School of Electronic Display Engineering, Hoseo University 20, Hoseo-ro 79beon-gil, Baebang-eup, Asan City 31499, Korea

* Correspondence: jingwang@aust.edu.cn (J.W.); cgjhun@hoseo.edu (C.G.J.)

Received: 30 June 2020; Accepted: 27 July 2020; Published: 7 August 2020

check for updates

Abstract: Based on various carbon nano materials, the ternary composite functionalized carbon nanotubes (FMWCNTs) @ carbon quantum dots (CQDs) @ polyaniline (PANI) was prepared by in-situ polymerization and hydrothermal method. The carbon-based material was made into an electrode sheet. The morphology and microscopic nanostructures were characterized by FTIR, field emission scanning electron microscopy and field emission transmission electron microscopy. Cyclic voltammetry and the galvanostatic charge discharge method was adapted to study the electrochemical properties of these active materials. Our results showed that the specific capacitance of FMWCNTs @ CQDs @ PANI was as high as 534 F/g, while it was 362 F/g, 319 F/g and 279 F/g for PANI @ FMWCNTs, PANI @ CQDs and polyaniline. This means that the specific capacitance of FMWCNTs @ CQDs @ PANI is increased by 47.5%, 67.4% and 91.4% comparing with the capacitance of PANI @ FMWCNTs, PANI @ CQDs and polyaniline, respectively. Moreover, the specific capacitance retention rate of the ternary active electrode after 1000 times of constant current charge and discharge cycle reached 86%, while it was 60% for PANI @ FMWCNTs, 72% for PANI @ CQDs and 65% for polyaniline.

Keywords: carbon quantum dots; functionalized multi-walled carbon nanotubes; polyaniline; composite electrode material; specific capacitance

---

1. Introduction

The research on carbon-doped materials has received more and more attention from academia. Especially, the interaction between conductive polymers, such as polyaniline (PANI) and carbon nanomaterials, such as multi-walled carbon nanotubes (MWCNTs) and carbon quantum dots (CQDs), has been researched hotspots since its discovery [1]. Due to the unique physical and chemical properties and their being easy to synthesize and obtain, MWCNTs are broadly applied for the preparation of various composite materials [2,3]. The electrical conductivity, thermal stability and mechanical strength of the composite, which included nanotubes and conjugated polymers, has been improved since plenty of work has been devoted to the development of see-through materials [4]. Especially after the combination of MWCNTs and conductive polymer PANI and other carbon nanomaterials, it can be used in supercapacitors [5] and effective adsorbents [6].

The rapid development of new supercapacitor has been widely favored with energy storage devices, which contains many advantages such as large charge and discharge current, high power density and long cycle life [6]. The electrochemical performance of supercapacitors mainly depends on the electrode materials [7,8], which are required to have a large specific surface area, excellent conductivity, rich pore size distribution and a stable structural system [9,10]. With the high specific surface area of carbon nanotubes (CNTs), relatively high electrical conductivity and significant chemical stability [11,12], it provides the possibility to prepare excellent electrochemically active materials [7]. However, the energy storage performance of CNTs is reduced dramatically by the defects of agglomeration resulting in bending and winding. Therefore, MWCNTs have been preliminarily functionalized. The bonds on the walls of MWCNTs are broken [13] and the specific surface area is increased with more active sites and better interface binding energy [14]. Therefore, the interaction between the surface and the conductive polymer modified layer is enhanced [2]. Among various conductive polymers, PANI has the advantages of easy preparation, low cost, reversibility [15–17] and good redox properties [17–20]. In addition, PANI is an ideal choice for preparing composite materials with good electrical and optical properties [1,21,22], as well as good environmental stability [23,24]. Nevertheless, the internal resistance and the volume expansion changes greatly in the process of using PANI, which makes the molecular chain of PANI breakdown and the performance of cycle stability insufficient [17,25]. In view of this, the performance of composite materials shows better performance than single components, based on the excellent synergistic effect of the combination of CNTs and PANI [1,26]. Similarly, with CNTs, the new type of carbon nanomaterial CQDs also have a large specific surface area [27] and good electrical conductivity [28]. In addition, it provides more space for electron transport and storage compared with CNTs.

In this experiment, FMWCNTs @ CQDs @ PANI, a new type of carbon matrix composite material, was compounded by PANI, FMWCNT and CQDs with in-situ polymerization and the hydrothermal method. After successful preparation, the composite material was fabricated into an electrode material, and its electrochemical performance was characterized.

2. Experimental

2.1. Materials and Preparation Method

We prepared a new composite electrode material by using CQDs, PANI and functionalized CNTs in this experiment. Under the power of 560 W, 200 mL CQDs were prepared by microwave method with carbon source glycerin (Sinopharm Chemical Reagent Co., Ltd., Shanghai, China) and trisodium phosphate (Fuchen Chemical Reagent Co., Ltd., Tianjin, China) and the reaction time was set at 25 min. The MWCNTs (Main Range of Diameter: 10–30 nm, Length: >2 µm, Purity: >97%, Ash: <3%, Special Surface Area: 160–200 m^2/g) were oxidized and refluxed for 7 h in concentrated nitric acid vapor at 110 °C to get FMWCNTs. The composite material PANI @ CQDs and PANI @ FMWCNTs was prepared by in-situ polymerization under acidic and ice bath conditions for 24 h, while the FMWCNTs @ CQDs was prepared with hydrothermal method at 150 °C for 3 h. Based on the composite material FMWCNTs @ CQDs, the ternary composite material FMWCNTs @ CQDs @ PANI was obtained by the following steps. First, the composite powder was synthesized with in-situ polymerization under acidic and ice bath conditions for 24 h. Second, it was rinsed with absolute ethanol and deionized water to neutral. Third, vacuum filtration, drying and grinding was completed in turn. To obtain the electrode sheet, FMWCNTs @ CQDs @ PANI, acetylene black and polyvinylidene fluoride (PVDF) were grinded with the mass ratio at 8:1:1. Then, appropriate N-methylpyrrolidone (NMP) was added dropwise according to the mass ratio and grinded for additional 15 min. After that, the grinded materials were evenly applied to a stainless-steel mesh (304 stainless steel wire mesh), pressed and dried.

2.2. Characterization

The type characteristics and material structure of the functional groups were studied and analyzed by conventional tests (7800–350 cm^{-1}) in FTIR (Nicolet iSr50, USA). The electrochemical performance of these materials was analyzed using an electrochemical workstation (CHI660e, Shanghai Chenhua Instrument Co., Ltd., Shanghai, China) to measure the CP curve, Cyclic voltammetry curve and constant current cycle curve.

3. Results and Discussion

3.1. FTIR Analysis

The FTIR spectra of the ternary composites FMWCNTs @ CQDs @ PANI, the composite materials PANI @ FMWCNTs and PANI @ CQDs, and the monolithic material PANI are shown in Figure 1. The absorption peaks of 3851 cm^{-1}, 3728 cm^{-1} and 3626 cm^{-1} in the composite material PANI @ FMWCNTs spectrum correspond to free OH, while the absorption peak 1655 cm^{-1} corresponds to C=O stretching vibration. The 1644 cm^{-1}, 1402 cm^{-1} and 1047 cm^{-1} of the composite material PANI @ CQDs spectrum correspond to C=O stretching vibration, O-H blending and C-O stretching, respectively [1,6,16,28–30]. It can be seen from the figure that the absorption peak is broad and strong for the composite sample, but a very weak spectrum for pure PANI, which may be related to the interaction between PANI and CNS, involves "charge transfer" [31]. When FMWCNTs and CQDs are attached to the surface of PANI, the intensity of the band will be increased in different degrees while introducing the characteristic functional groups. For the ternary composite FMWCNTs @ CQDs @ PANI, the functional group type and peak intensity have been strengthened, and the absorption peak is also clearer. In the FTIR spectrum, the composite material's spectrum contains the characteristic peaks of PANI, indicating that the generated PANI is wrapped on FMWCNTs and CQDs after polymerization with the aniline monomer. The inhibited growth and suppressed atomic vibration resulted in some absorption peaks in the composite material spectrum being similar, and absorption peaks of hydroxyl functional groups also appeared in the PANI @ FMWCNTs spectrum. Considering all the factors, the composite material was proven to be successfully prepared.

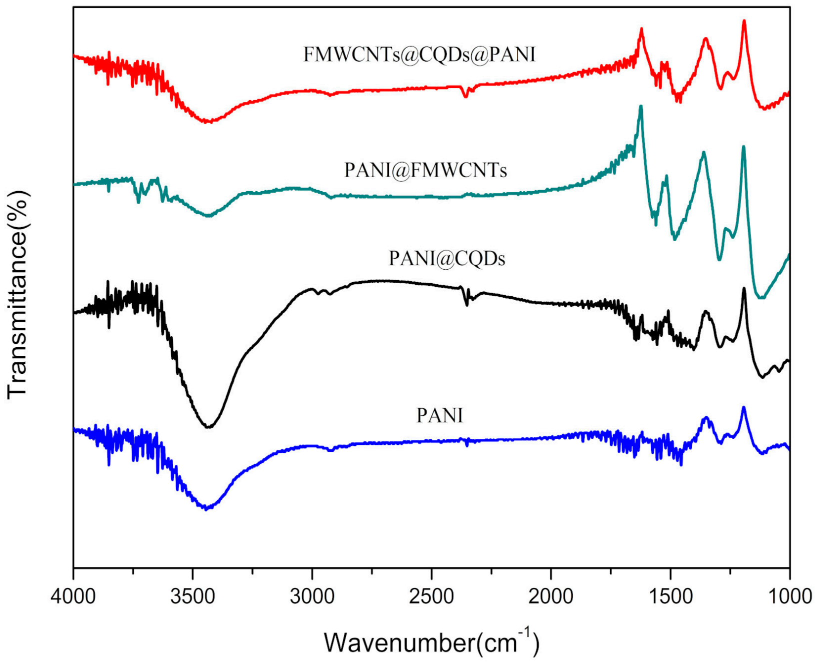

Figure 1. FTIR spectra of FMWCNTs @ CQDs @ PANI, PANI @ FMWCNTs, PANI @ CQDs and PANI.

3.2. Electrochemical Performance

Figure 2 shows the constant current charge and discharge curves of the electrode sheets prepared by the monolithic material PANI, the composite materials PANI @ CQDs and PANI @ FMWCNTs, and the ternary composite material FMWCNTs @ CQDs @ PANI in a 1 M H_2SO_4 electrolyte. At a current density of 0.5 A/g, the specific capacitances of the four materials were measured at 279 F/g, 319 F/g, 362 F/g, and 534 F/g, respectively. Compared to PANI, PANI @ CQDs, and PANI @ FMWCNTs, the specific capacitance of FMWCNTs @ CQDS @ PANI was increased by 91.4%, 67.4% and 47.5%, respectively. What is more, the capacitance retention rate of FMWCNTs @ CQDS @ PANI reached 86% after 1000 cycles, which was higher than 72% of PANI @ CQDs, 60% of PANI @ FMWCNTs and 65% of pure PANI. In addition, it can be seen from the constant current charge–discharge curves of the electrode materials PANI, PANI @ CQDs and PANI @ FMWCNTs that their charging time is much longer than the discharge time, while the constant current charge and discharge curve of the ternary electrode material shows a near perfect state—almost symmetry [32]. This phenomenon reflects the synergistic effect between monomers [1,29]. More importantly, compared with PANI, PANI @ CQDS and PANI @ FMWCNTs, FMWCNTs @ CQDS @ PANI electrode has obvious linear deviation on GCD curve, indicating that FMWCNTs @ CQDs @ PANI has significant pseudo capacitance characteristic [16]. The reason for this is likely to be manifested in two aspects: (I) as the nature of the material itself is not good enough, the dispersion is poor in the process of preparing the electrode material, and the specific surface area is limited, thereby making its electrochemical performance is affected; (II) because of its large electrical resistance, the electrochemical reversibility is poor, which affects the cycle life and capacity attenuation of the electrode.

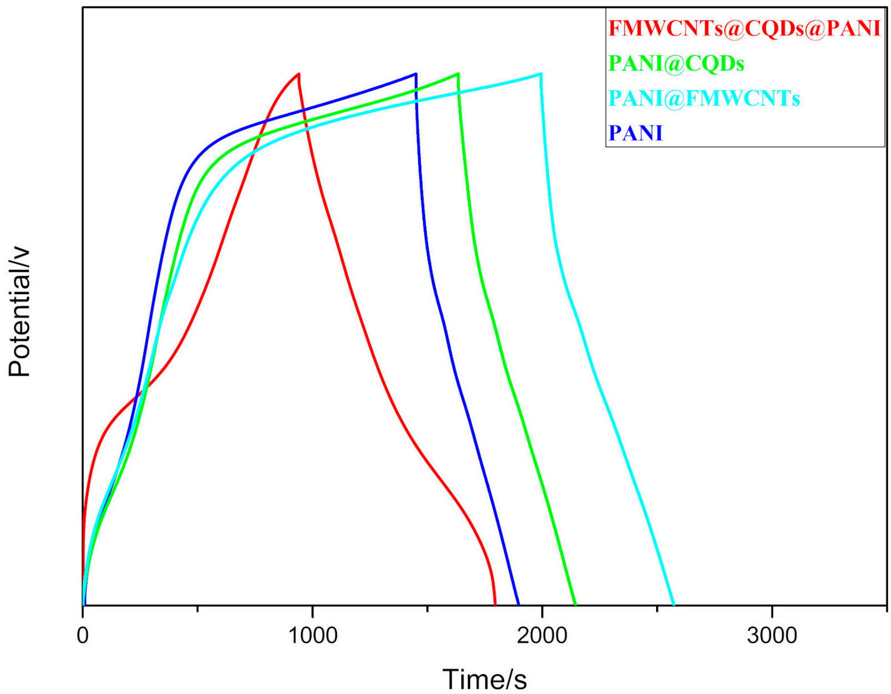

Figure 2. Constant current charge and discharge curves of PANI, PANI @ CQDs, PANI @ FMWCNTs and FMWCNTs @ CQDs @ PANI in 1 M H_2SO_4 electrolyte.

The curves obtained by charging and discharging the four electrode materials PANI, PANI @ CQDs, PANI @ FMWCNTs and FMWCNTs @ CQDs @ PANI in a current density of 5 A/g and 1 M H_2SO_4 electrolyte for 20 cycles are shown in Figure 3a–d. It can be seen that the time taken for the 20 cycles of the PANI electrode is only 300 s, while the time taken for the 20 cycles of the PANI @ CQDs electrode and PANI @ FMWCNTs electrode is more than 1000 s and 1200 s separately. There is no significant difference between the two composite materials. However, the time taken for the 20-cycle of the ternary active electrode has reached more than 2750 s, which is more than twice the time spent on the binary active electrode. In addition, the specific capacitance decreases with the increase in the number of cycles [33]. There are two possible reasons: (I) the electrolyte decomposes on the surface of the electrode material during the electrolysis process [34]; (II) the dissolution and stripping of the active material and the reduction in the active center during the electrolysis process [35].

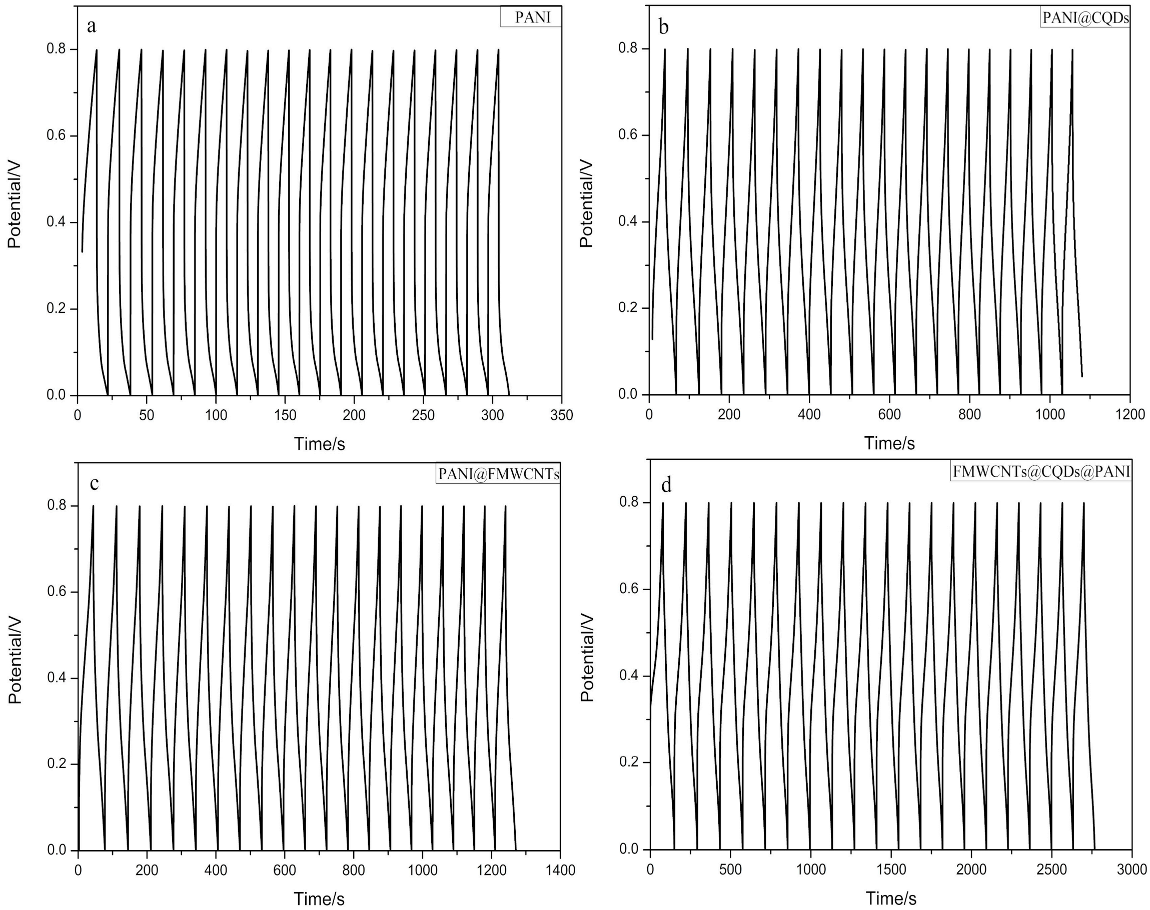

Figure 3. Time curves of (**a**) PANI, (**b**) PANI @ CQDs, (**c**) PANI @ FMWCNTs and (**d**) FMWCNTs @ CQDs @ PANI constant current charge and discharge cycle for 20 periods.

According to Formula (1), there is a direct relationship between the discharge time and the specific capacitance. Therefore, it is concluded that the electrical activity of ternary composite is better than that of PANI, PANI @ CQDs and PANI @ FMWCNTs.

$$C_s = \frac{I\Delta t}{m(U - \Delta U)} \quad (1)$$

For its specific capacitance retention ratio (Figure 4), it can be seen that the composite material PANI @ FMWCNTs has poor performance of the electrode material after multiple charge and discharge comparing PANI @ CQDs, even lower than the retention rate of pure PANI. According to the cyclic voltammetry curve in Figure 5, there is a significant redox peak. The possible reason is a sharp decay of the cycle life of the electrode material, as that the electrolyte has a large irreversible capacity during multiple charge and discharge processes, and the embedding of solvent molecules directly leads to the serious collapse of the electrode material.

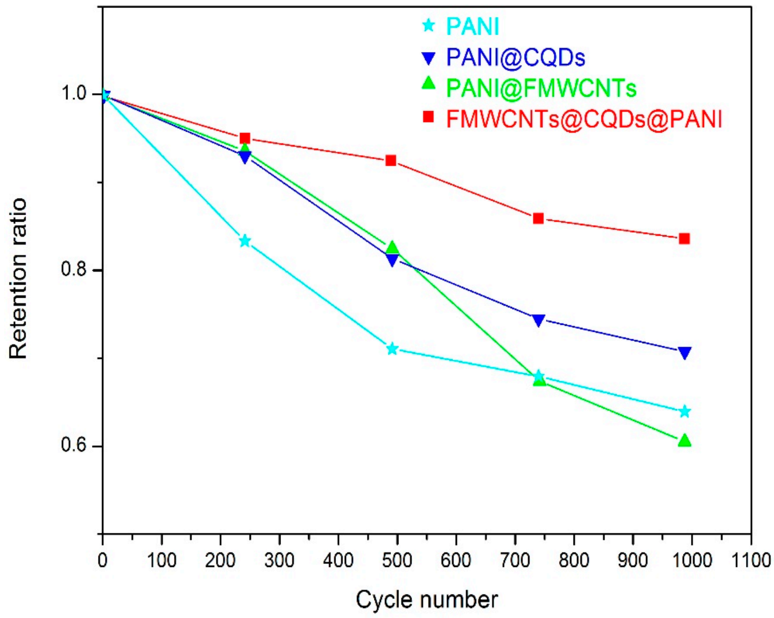

Figure 4. Retention rates of PANI, PANI @ CQDs, PANI @ FMWCNTs and FMWCNTs @ CQDs @ PANI under different number of cycles.

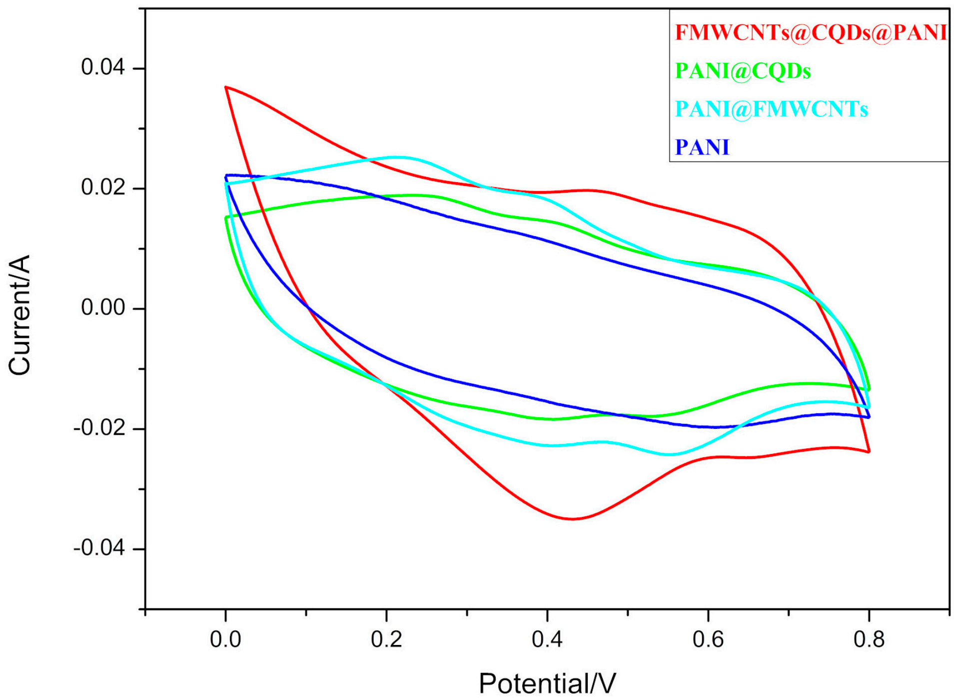

Figure 5. Cyclic voltammetry curves of PANI, PANI @ CQDs, PANI @ FMWCNTs and FMWCNTs @ CQDs @ PANI.

To further compare the electrochemical capacitive behaviors of PANI, PANI @ CQDs, PANI @ FMWCNTs and FMWCNTs @ CQDs @ PANI electrodes, CV tests were carried out at 10 mv·s^{-1}, as shown in Figure 5. It can be seen from the figure that there is a significant redox peak in the FMWCNTs @ CQDs @ PANI curve in the interval of 0.4–0.5 V, indicating that the redox reaction is reversible. It can also be observed that the cyclic voltammetry curve is approximately embodied as an isosceles triangle, which reflects the combination of the electric double layer capacitance and the tantalum capacitance of the composite material, good reversibility [32,36]. It is also obvious that

FMWCNTs @ CQDs @ PANI electrode has much higher redox peak current, suggesting increased specific capacitance. There is also a significant redox peak in the PANI @ CQDs and PANI @ FMWCNTs cyclic voltammetry curve. The two types of electrodes show the same pair of redox peaks, which are attributed to redox transition of PANI between CQDs and FMWCNTs [37]. In comparison, the redox peak in the pure PANI is very weak [38], indicating that the redox reaction is less reversible. Combined with the conclusions obtained in Figure 2, the electrical activity and reversibility of the PANI @ FMWCNTs electrode in the early stage are better than those in the later stage. In addition, from the active area of the curve, the electrical activity of the ternary active material is better than the composite materials PANI @ CQDs and PANI @ FMWCNTs, as well as pure polyaniline, with strong energy storage capacity [32]. Furthermore, it shows that the compounding of three active materials has been successful. Therefore, the conclusion about the specific capacitance obtained in the constant current charge and discharge curve of Figure 2 was verified: ternary active electrode > binary active electrode > pure polyaniline.

Figure 6 shows the cyclic voltammetric curves of PANI, PANI @ CQDS, PANI @ FMWCNTs and FMWCNTs @ CQDs @ PANI at a series of scanning rate ranging from 5 to 50 mv·s^{-1}. It can be seen that: (I) the specific capacitance decreases with the increase in scanning rate (Table 1), which may be due to the superior charge mobilization per unit time [39]; (II) the response current increases with the increase in scanning rate, which shows that the composite has good electrochemical reversibility and high-power characteristics [32].

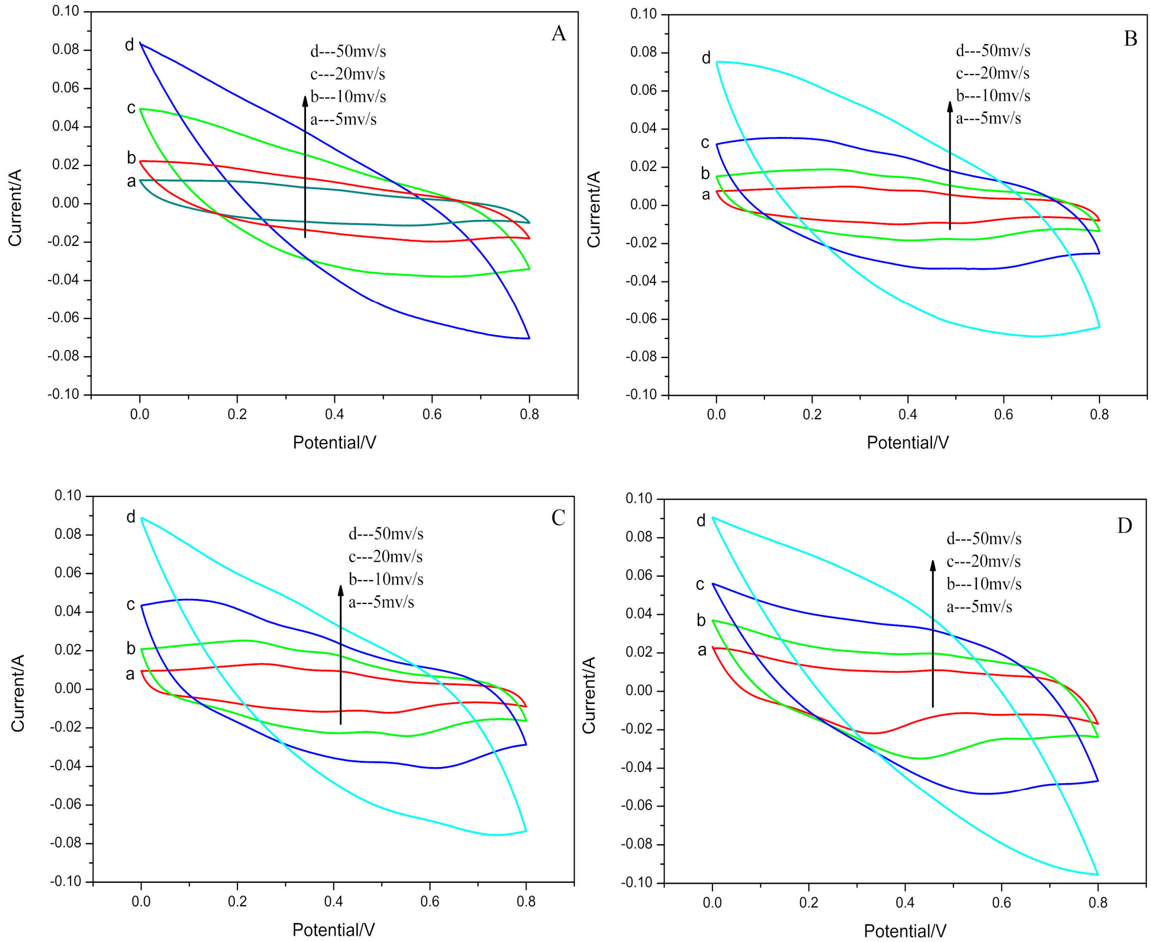

Figure 6. CV curves at different scan rates of (**A**) pure PANI, (**B**) PANI @ CQDs, (**C**) PANI @ FMWCNTs, and (**D**) FMWCNTs @ CQDs @ PANI.

Table 1. Specific capacitance of pure PANI, PANI @ CQDs, PANI @ FMWCNTs, and FMWCNTs @ CQDs @ PANI nanocomposites at different scan rates.

Sample/Scan Rates	5 mv/s	10 mv/s	20 mv/s	50 mv/s
PANI	185.24 F/g	155.12 F/g	157 F/g	100.75 F/g
PANI @ CQDs	245.45 F/g	236.36 F/g	215.34 F/g	162.73 F/g
PANI @ FMWCNTs	293.98 F/g	296.30 F/g	251.16 F/g	169.44 F/g
FMWCNTs @ CQDs @ PANI	507.81 F/g	441.41 F/g	355.47 F/g	224.22 F/g

4. Conclusions

In this experiment, FTIR, electron microscopy and electrochemical studies have shown that the preparation of ternary composite electrode materials has been successful. After the polymerization of carbon nanomaterials and conductive polymer PANI, its electrochemical performance was greatly improved, especially in the constant current cycle charge and discharge curve. Its specific capacitance is much higher than pure PANI and composite electrode materials, and the cycle stability is also greatly improved. On the other hand, the doped composite material effectively improves the performance degradation caused by agglomeration, slows down the energy decay, enhances its dispersibility in solution, increases the specific surface area, improves its stability, and further enhances its electrical activity and reversibility. In addition, a composite material composed of an electroactive material with a high specific surface area and a carbon material significantly increases the energy density of the electrode material and is also a major cause of an increase in specific capacitance. Finally, during the electrolysis process, the problem of the collapse of the electrode sample after PANI composite requires further study.

Author Contributions: Conceptualization, J.W., C.G.J.; Methodology, Y.C.; Software, Y.C.; Validation, J.W., Y.C. and Z.H.; Formal analysis, Y.C., Y.G. and T.H.; Investigation, J.W., C.G.J. and Y.C.; Data curation, Y.C., Y.G. and G.D.; Writing—original draft, Y.C.; Writing—review and editing, J.W., C.G.J., Y.C., Z.H. and Y.G.; Visualization, J.W. and Y.C.; Supervision, J.W.; Project administration, J.W.; Funding acquisition, J.W. and C.G.J.; All authors have read and agreed to the final publication. All authors have read and agreed to the published version of the manuscript.

Funding: This research was supported by the AURI (Korea Association of University), Research Institute and Industry) grant funded by the Korea Government (MSS: Ministry of SMEs and Startups). (No. 2020, HRD program for S2924363), and this work was financially supported by National Natural Science Foundation of China (51002002) and open fund of Key Laboratory of optical functional inorganic materials of Chinese Academy of Sciences (No KLTOIM201609).

Conflicts of Interest: The authors declare no conflict of interest.

References

1. Xu, F.; Jamal, R.; Ubul, A.; Shao, W.; Abdiryim, T. Characterization and electrochemical properties of poly(aniline-co-o-methoxyaniline)/multi-walled carbon nanotubes composites synthesized by solid-state method. *Fibers Polym.* **2013**, *14*, 8–15. [CrossRef]
2. Dyachkova, T.P.; Anosova, I.V.; Tkachev, A.G.; Chapaksov, N.A. Synthesis of composites from functionalized carbon nanotubes and polyaniline. *Inorg. Mater. Appl. Res.* **2018**, *9*, 305–310. [CrossRef]
3. Zhou, Y.; Qian, W.; Huang, W.; Liu, B.; Lin, H.; Dong, C. Carbon nanotube-graphene hybrid electrodes with enhanced thermo-electrochemical cell properties. *Nanomaterials* **2019**, *9*, 1450. [CrossRef]
4. Abalyaeva, V.V.; Vershinin, N.N.; Shul'ga, Y.M.; Efimov, O.N. The composites of polyaniline with multiwall carbon nanotubes: Preparation, electrochemical properties, and conductivity. *Russ. J. Electrochem.* **2009**, *45*, 1266–1275. [CrossRef]
5. Nikzad, L.; Vaezi, M.R.; Yazdani, B. Synthesis of carbon nanotube–Poly aniline nano composite and evaluation of electrochemical properties. *Int. J. Mod. Phys. Conf. Ser.* **2012**, *5*, 527–535. [CrossRef]

6. Agyemang, F.O.; Tomboc, G.M.; Kwofie, S.; Kim, H. Electrospun carbon nanofiber-carbon nanotubes coated polyaniline composites with improved electrochemical properties for supercapacitors. *Electrochim. Acta* **2018**, *259*, 1110–1119. [CrossRef]
7. Grodzka, E.; Pieta, P.; Dłużewski, P.; Kutner, W.; Winkler, K. Formation and electrochemical properties of composites of the C_{60}–Pd polymer and multi-wall carbon nanotubes. *Electrochim. Acta* **2009**, *54*, 5621–5628. [CrossRef]
8. Kurra, N.; Jiang, Q.; Alshareefn, H.N. A general strategy for the fabrication of high performance microsupercapacitors. *Nano Energy* **2015**, *16*, 1–9. [CrossRef]
9. Chen, H.S.; Drag, Y. Progress in electrical energy storage system: A critical review. *Prog. Nat. Sci.* **2009**, *19*, 291–312. [CrossRef]
10. Li, Y.L.; Zheng, Y.Y. Preparation and electrochemical properties of polyaniline/reduced graphene oxide composites. *J. Appl. Polym. Sci.* **2018**, *135*, 235–262. [CrossRef]
11. Liu, L.; Niu, Z.; Chen, J. Flexible supercapacitors based on carbon nanotubes. *Chin. Chem. Lett.* **2018**, *29*, 571–581. [CrossRef]
12. Pei, X.Y.; Mo, D.C.; Lyu, S.S.; Zhang, J.H.; Fu, Y.X. Synthesis of MnCO(3)/Multiwalled carbon nanotube composite as anode material for lithium-ion batteries. *J. Nanosci. Nanotechnol.* **2019**, *19*, 5743–5749. [CrossRef] [PubMed]
13. Wulandari, S.A.; Widiyandari, H.; Subagio, A. Synthesis and characterization carboxyl functionalized Multi-Walled Carbon Nanotubes (MWCNT-COOH) and NH_2 functionalized Multi-Walled Carbon Nanotubes ($MWCNTNH_2$). *J. Phys. Conf. Ser.* **2018**, *1025*, 12005. [CrossRef]
14. Aziz, S.A.A.; Mazlan, S.A.; Ismail, N.I.N.; Choi, S.B. Implementation of functionalized multiwall carbon nanotubes on magnetorheological elastomer. *J. Mater. Sci.* **2018**, *53*, 10122–10134. [CrossRef]
15. Zhang, Y.; Zhou, M.; Dou, C.; Ma, G.; Wang, Y.; Feng, N.; Wang, W.; Fang, L. Synthesis and biocompatibility assessment of polyaniline nanomaterials. *J. Bioact. Compat. Polym.* **2018**, *34*, 16–24. [CrossRef]
16. Zhou, H.; Zhi, X.; Zhai, H.-J. A facile approach to improve the electrochemical properties of polyaniline-carbon nanotube composite electrodes for highly flexible solid-state supercapacitors. *Int. J. Hydrogen Energy* **2018**, *43*, 18339–18348. [CrossRef]
17. Chen, S.; Liu, B.; Wang, Y.; Cheng, H.; Zhang, X.; Xu, S.; Liu, H.; Liu, W.; Hu, C. Excellent electrochemical performances of intrinsic polyaniline nanofibers fabricated by electrochemical deposition. *J. Wuhan Univ. Technol. Mater Sci. Ed.* **2019**, *34*, 216–222. [CrossRef]
18. Robertson, J.; Dalton, J.; Wiles, S.; Gizdavic-Nikolaidis, M.; Swift, S. The tuberculocidal activity of polyaniline and functionalised polyanilines. *PeerJ* **2016**, *4*, e2795. [CrossRef]
19. Koluaçik, E.; Karabiberoğlu, Ş.U.; Dursun, Z. Electrochemical determination of serotonin using pre-treated multi-walled carbon nanotube-polyaniline composite electrode. *Electroanalysis* **2018**, *30*, 2977–2987. [CrossRef]
20. Oueiny, C.; Berlioz, S.; Perrin, F.-X. Carbon nanotube-polyaniline composites. *Prog. Polym. Sci.* **2014**, *39*, 707–748. [CrossRef]
21. Bharadiya, P.; Jainm, R.; Chaudhari, V.; Mishra, S. Graphene oxide-wrapped polyaniline nanorods for supercapacitor applications. *Polym. Compos.* **2019**, *40*, E1716–E1724. [CrossRef]
22. Zhou, L.; Qiao, M.; Zhang, L.; Sun, L.; Zhang, Y.; Liu, W. Green and efficient synthesis of carbon quantum dots and their luminescent properties. *J. Lumin.* **2019**, *206*, 158–163. [CrossRef]
23. Namdari, P.; Negahdari, B.; Eatemadi, A. Synthesis, properties and biomedical applications of carbon-based quantum dots: An updated review. *Biomed. Pharm.* **2017**, *87*, 209–222. [CrossRef]
24. Ladrón de Guevara, A.; Boscá, A.; Pedrós, J.; Climent-Pascual, E.; De Andrés, A.; Calle, F.; Martínez, J. Reduced graphene oxide/polyaniline electrochemical supercapacitors fabricated by laser. *Appl. Surf. Sci.* **2019**, *467*, 691–697. [CrossRef]
25. Armes, S.P.; AIdissi, M. Potassium iodate oxidation route to polyaniline: An optimization study. *Polymer* **1991**, *32*, 2043–2048. [CrossRef]
26. Feng, W.; Bai, X.D.; Lian, Y.Q.; Liang, J.; Wang, X.G.; Yoshino, K. Well-aligned polyaniline/carbon-nanotube composite films grown by in-situ aniline polymerization. *Carbon* **2003**, *41*, 1551–1557. [CrossRef]
27. Kovalyshyn, Y.; Konovska, M.; Milanese, C.; Saldan, I.; Serkiz, R.; Pereviznyk, O.; Reshetnyak, O.; Kuntyi, O. Electrochemical properties of the composites synthesized from polyaniline and modified mwcnt. *Chem. Chem. Technol.* **2017**, *11*, 261–269. [CrossRef]
28. Mezdour, D. Dielectric properties of polyaniline composites. *Spectrosc. Lett.* **2017**, *50*, 214–219. [CrossRef]

29. Faraji, M.; Mohammadzadeh, A.H. Flexible free-standing polyaniline/graphene/carbon nanotube plastic films with enhanced electrochemical activity for an all-solid-state flexible supercapacitor device. *New J. Chem.* **2019**, *43*, 4539–4546. [CrossRef]
30. Trchová, M.; Matějka, P.; Brodinová, J.; Kalendova, A.; Prokeš, J.; Stejskal, J. Structural and conductivity changes during the pyrolysis of polyaniline base. *Polym. Degrad. Stab.* **2006**, *91*, 114–121. [CrossRef]
31. Plonska-brzezinska, M.E.; Breczko, J.; Palys, B.; Echegoyen, L. The electrochemical properties of nanocomposite films obtained by chemical in situ polymerization of aniline and carbon nanostructures. *Chemphyschem* **2013**, *14*, 116–124. [CrossRef] [PubMed]
32. Miao, F.; Shao, C.; Li, X.; Wang, K.; Lu, N.; Liu, Y. Electrospun Carbon nanofibers/carbon nanotubes/polyaniline ternary composites with enhanced electrochemical performance for flexible solid-state supercapacitors. *ACS Sustain. Chem. Eng.* **2016**, *4*, 1689–1696. [CrossRef]
33. Bhattacharya, P.; Dhibar, S.; Kundu, M.K.; Hatui, G.; Das, C.K. Graphene and MWCNT based bi-functional polymer nanocomposites with enhanced microwave absorption and supercapacitor property. *Mater. Res. Bull.* **2015**, *66*, 200–212. [CrossRef]
34. Wang, Y.-G.; Cheng, L.; Xia, Y.-Y. Electrochemical profile of nano-particle CoAl double hydroxide/active carbon supercapacitor using KOH electrolyte solution. *J. Power Sources* **2006**, *153*, 191–196. [CrossRef]
35. Zheng, Y.-Z.; Ding, H.-Y.; Zhang, M.-L. Preparation and electrochemical properties of nickel oxide as a supercapacitor electrode material. *Mater. Res. Bull.* **2009**, *44*, 403–407. [CrossRef]
36. Vedhanarayanan, B.; Huang, T.-H.; Lin, T.-W. Fabrication of 3D hierarchically structured carbon electrode for supercapacitors by carbonization of polyaniline/carbon nanotube/graphene composites. *Inorg. Chim. Acta* **2019**, *489*, 217–223. [CrossRef]
37. Liang, J.S.; Su, S.J.; Fang, X.; Wang, D.Z.; Xu, S.C. Electrospun fibrous electrodes with tunable microstructure made of polyaniline/multi-walled carbon nanotube suspension for all-solid-state supercapacitors. *Mater. Sci. Eng. B* **2016**, *211*, 61–66. [CrossRef]
38. Chaudhari, S.; Sharma, Y.; Archana, P.S.; Jose, R.; Ramakrishna, S.; Mhaisalkar, S.; Srinivasan, M. Electrospun polyaniline nanofibers web electrodes for supercapacitors. *J. Appl. Polym. Sci.* **2013**, *129*, 1660–1668. [CrossRef]
39. Dhibar, S.; Sahoo, S.; Das, C.K. Copper chloride-doped polyaniline/multiwalled carbon nanotubes nanocomposites: Superior electrode material for supercapacitor applications. *Polym. Compos.* **2013**, *34*, 517–525. [CrossRef]